

Self-Aggregation Properties of Ionic Liquid 1,3-Didecyl-2-methylimidazolium Chloride in Aqueous Solution: From Spheres to Cylinders to Bilayers

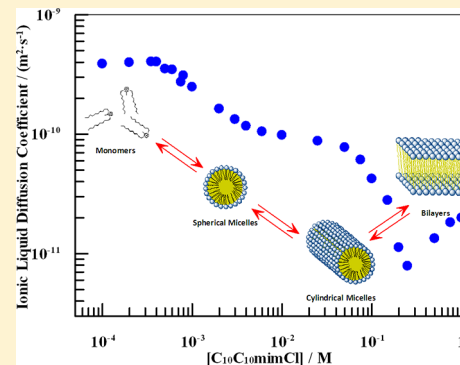
Maria Figueira-González,[†] Vitor Francisco,[†] Luis García-Río,^{*,†} Eduardo F. Marques,[‡] Mercedes Parajó,[†] and Pedro Rodríguez-Dafonte^{*,†}

[†]Centro Singular de Investigación en Química Biológica y Materiales Moleculares, Department of Physical Chemistry, University of Santiago de Compostela, 15782, Santiago de Compostela, Spain

[‡]Centro de Investigação em Química, Department of Chemistry and Biochemistry, Faculty of Sciences, University of Porto, Rua do Campo Alegre, 687, 4169-007 Porto, Portugal

Supporting Information

ABSTRACT: The self-aggregation behavior of the double-chained ionic liquid (IL) 1,3-didecyl-2-methylimidazolium chloride ($[C_{10}C_{10}\text{mim}]Cl$) in aqueous solution has been investigated with a number of different experimental techniques. Two cmc values (cmc_1 and cmc_2) are obtained from conductivity measurements. The fraction of neutralized charge on the micellar surface suggests that cmc_1 corresponds to the formation of spherical micelles and cmc_2 to the transition from spherical to cylindrical micelles. Data obtained from fluorescence spectroscopy (using pyrene and Nile red as chemical probes), fluorescence anisotropy (using rhodamine B as probe), and chemical shift ^1H NMR (in $D_2\text{O}$) provide a picture that is also consistent with a sphere-to-cylinder transition. This structural change is further confirmed by diffusion-ordered NMR spectroscopy (DOSY), from the self-diffusion coefficients for surfactant unimer and aggregates. Furthermore, a third evolution from cylindrical micelles to bilayer aggregates is proposed from the analysis of diffusion coefficients at high surfactant concentration ($[\text{IL}] > 0.2 \text{ M}$). Phase scanning experiments performed with polarized light microscopy clearly demonstrate the presence of a lamellar liquid crystalline phase at very high IL concentration, thus confirming the coexistence of bilayer structures with elongated micelles, found at lower concentration. Additionally, $[C_{10}C_{10}\text{mim}]Cl$ micelles are proposed as novel reaction media, as evidenced by the solvolysis reaction of 4-methoxybenzenesulfonyl chloride (MBSC).



INTRODUCTION

Ionic liquids (ILs) are salts, composed solely of ions with melting points below 100 °C,¹ that present unique properties^{2–4} and applications.^{5–9} Amphiphilic ILs are constituted by a charged hydrophilic headgroup and one or more hydrophobic tails. There is an evident structural similarity between frequently used traditional ionic surfactants (salts) and long-chain ILs (liquid salts), and hence, ILs are also able to self-aggregate as micelles in aqueous solution, like common ionic amphiphiles. Long-chain ILs composed of the 1-alkyl-3-methylimidazolium cation ($[C_n\text{mim}]^+$) are among this novel type of amphiphiles that have been studied in recent years. Fluorescence, interfacial tension, and ^1H NMR techniques have been used in order to determine the nature of the self-aggregation behavior of $[C_n\text{mim}]^+$ -based ILs in water varying the counterion (Cl^- , PF_6^- , and NTf_2^-) and the alkyl chain length, n , in the range 2–14.¹⁰ For $[C_n\text{mim}]Cl$ ILs, there is a good correlation between the Gibbs energy of micellization and n , with the type of dependence being similar to that shown by alkyltrimethylammonium and alkylammonium chloride families. Isothermal titration microcalorimetry has been used to

obtain the thermodynamic parameters of micellization for $[C_{12}\text{mim}]Br$, $[C_{14}\text{mim}]Br$, and $[C_{16}\text{mim}]Br$, asserting that the process of micellization is entropy-driven.¹¹ Pyridinium-based amphiphilic ILs have been prepared in order to investigate the relation between their aggregation and the antimicrobial activity.¹²

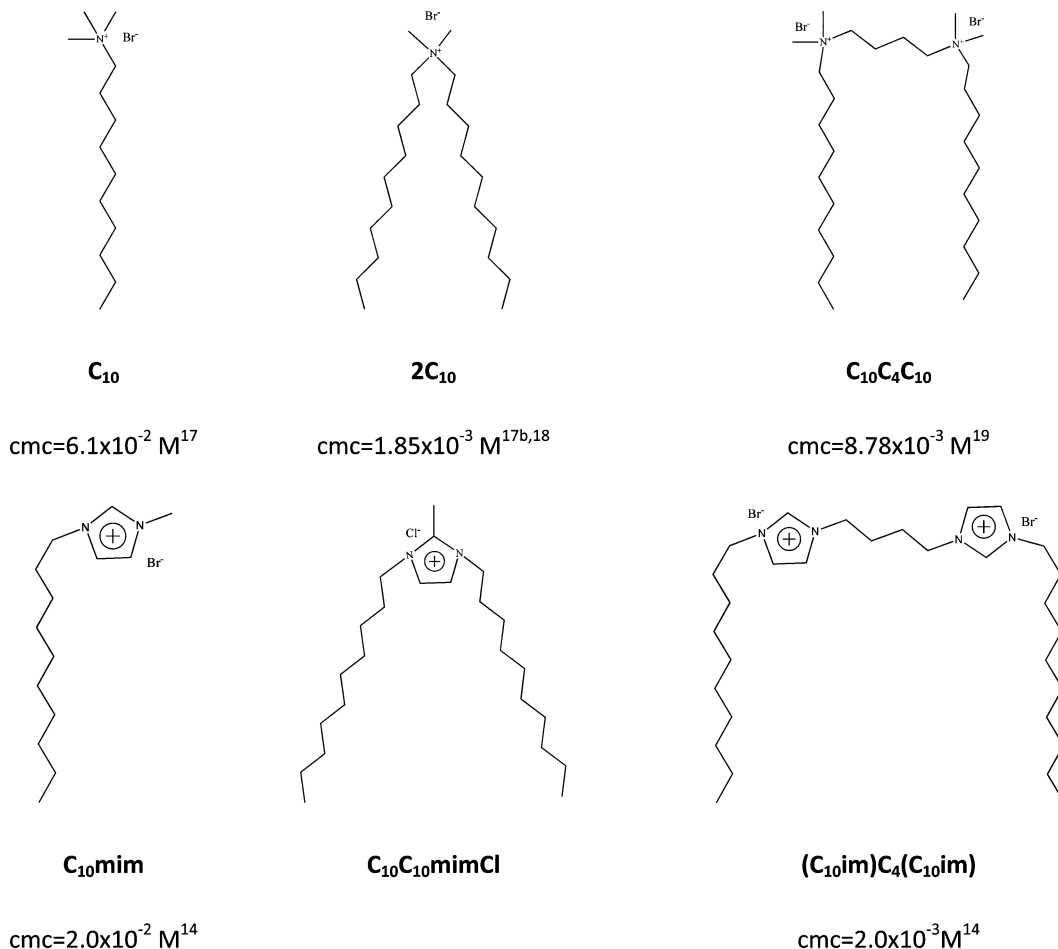
A different class of IL-based surfactants is that containing double chains or a dimeric structure similar to gemini surfactants. The length of the covalent spacers between headgroups, and the length of the chains, can significantly affect the properties of gemini-type ILs. For instance, studies on the physicochemical properties of 1,4-bis(3-tetradecylimidazolium-1-yl) butane bromide show that this novel gemini ionic liquid possesses higher thermal stability, lower critical micelle concentration, and larger d -spacing of crystal structure than the homologous ionic liquid with a single long chain.¹³ Using surface tensiometry, the self-aggregation of six dicationic

Received: November 30, 2012

Revised: January 29, 2013

Published: February 5, 2013

Scheme 1



imidazolium-based ILs with structures resembling gemini and bolaform surfactants have been reported.¹⁴ The aggregation behavior of imidazolium-based gemini surfactants has been explored and compared with the equivalent surfactants possessing ammonium headgroups.¹⁵ In the case of the IL, upon increasing the spacer chain length s , the cmc increases. This trend can be explained in terms of conformational changes and progressive looping of the spacer into the micellar interior upon increasing s . In contrast, for conventional *bis*-quat ammonium-based cationic gemini surfactants, the cmc has a non-monotonic dependence with s , going through a maximum at $s = 6$.¹⁶

In this work, we investigate the self-assembling properties of the double-chained IL designated as 1,3-didecyl-2-methylimidazolium chloride ($[\text{C}_{10}\text{C}_{10}\text{mim}] \text{Cl}$). This IL can be regarded as having a molecular structure intermediate between that of a single-chained amphiphile and of a double-chained gemini amphiphile. Scheme 1 shows the molecular structure of six surfactants with alkyl chains of 10 carbons. The cmc of decyl trimethylammonium bromide (C_{10}) is higher than that of didecyl dimethylammonium bromide (2C_{10}) and of the dicationic gemini surfactant ($\text{C}_{10}\text{C}_4\text{C}_{10}$).^{17–19} The order of cmc values, $2\text{C}_{10} < \text{C}_{10}\text{C}_4\text{C}_{10} < \text{C}_{10}$, shows that micellization is favored for molecules with a double-chained structure. For the current surfactant, $\text{C}_{10}\text{C}_{10}\text{mimCl}$, one can anticipate a similar trend, with its cmc being lower than that of decyl methylimidazolium, C_{10}mim , and gemini IL $(\text{C}_{10}\text{im})\text{C}_4(\text{C}_{10}\text{im})$. From the values of the $\text{C}_{10}/\text{C}_{10}\text{mim}$ and $\text{C}_{10}\text{C}_4\text{C}_{10}/(\text{C}_{10}\text{im})$

$\text{C}_4(\text{C}_{10}\text{im})$ cmc ratios, which are 3.0 and 4.4, respectively, one estimates a cmc value for $\text{C}_{10}\text{C}_{10}\text{mimCl}$ of the order of $(4–6) \times 10^{-4} \text{ M}$. Data from conductometry and NMR obtained in this work demonstrate in fact the existence of two cmc values for $\text{C}_{10}\text{C}_{10}\text{mimCl}$, the first one (cmc_1) in agreement with the value expected from the above-mentioned considerations and the second one (cmc_2) related to a change in the shape of the aggregates. Furthermore, NMR self-diffusion data together with phase scanning experiments under polarized light show also a third transition from elongated micelles to bilayers. From a phase behavior point of view, this happens when the micelle isotropic solution is crossed to a two-phase region of micelle solution and a lamellar liquid-crystalline phase. Finally, and due to the interest of ILs as new reaction media, we have carried out the kinetic study of the solvolysis reaction of 4-methoxybenzenesulfonyl chloride in the presence of micelles of $\text{C}_{10}\text{C}_{10}\text{mimCl}$.

EXPERIMENTAL SECTION

The ionic liquid $[\text{C}_{10}\text{C}_{10}\text{mim}] \text{Cl}$ was obtained from the manufacturer Io-li-tec (Germany) with a mass fraction purity better than 0.98 and used as received. In an effort to avoid the absorption of atmospheric water, the compound was stored under vacuum in a desiccator filled with molecular sieves, and only fresh samples were used.

The solvatochromic probe 2,6-dichloro-4-(2,4,6-triphenyl-1-pyridinio)phenolate [$E_{\text{T}}(33)$], also known as Reichardt's betaine dye, was obtained from Sigma-Aldrich and used as received.

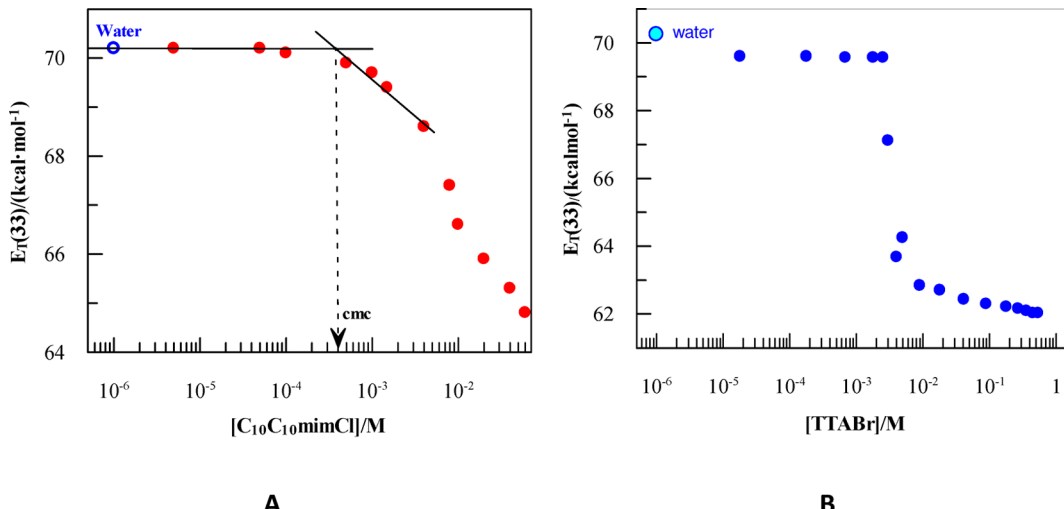


Figure 1. (A) Variation of the E_T value with $[\text{C}_{10}\text{C}_{10}\text{mim}] \text{Cl}$ concentration in aqueous solution at 25°C . (B) Variation of the E_T value with TTABr concentration in aqueous solution at 25°C .

UV-vis absorbance spectra were recorded on a Cary 500 scan UV-vis-NIR spectrophotometer fitted with thermostated cell holders. The polarity was expressed on the E_T scale, one of the most widely used empirical solvent parameter scales. The final concentration of the dye was 0.30 mM.

Conductivity experiments were carried out using a Crison conductimeter GLP32. The conductimeter was calibrated with KCl solutions supplied by Crison. Milli Q water was used in the preparation of the $[\text{C}_{10}\text{C}_{10}\text{mim}] \text{Cl}$ solutions. The temperature was kept constant to within $\pm 0.1^\circ\text{C}$ by passing thermostated water through a jacketed vessel containing the solution.

Steady-state fluorescence experiments were recorded using a Cary Eclipse instrument. The fluorescent probes used, Nile red, pyrene, and rhodamine B, were purchased from Aldrich. All of these chemicals are of the highest available purity and were used without further purification. The fluorescence spectra of pyrene, Nile red, and rhodamine B were measured with an excitation wavelength of 334, 575, and 554 nm, respectively. All emission spectra measured were corrected for emission monochromator response and were background-subtracted using appropriate blanks. Slits and rate of acquisition were chosen for a convenient signal-to-noise ratio. For pyrene, the intensities of the first (I_1) and third (I_3) vibronic bands in emission spectra located around 373 and 384 nm, respectively, were measured and used to determine the I_1/I_3 ratio. This ratio is very sensitive to changes in the polarity of the solvent.²⁰ With the same aim, for Nile red, we monitored the change in the maximum wavelength of emission.

The fluorescence anisotropy value was determined, from the emission spectra of rhodamine B, as

$$r = \frac{G \cdot I_{VV} - I_{VH}}{G \cdot I_{VV} + 2I_{VH}} \quad (1)$$

where the subscripts of the fluorescence intensity values (I) refer to vertical (V) and horizontal (H) polarizer orientations. The instrumental correction factor G ($G = I_{HH}/I_{HV}$), required for the L-format configuration, was automatically determined by the software supplied by the manufacturer. The steady-state polarization is related to the rotational relaxation time of a rigid sphere by the Perrin equation.²¹ Changes in microstructure are reflected in changes in viscosity around the probe, and hence in r values.²²

NMR measurements were performed on a 400 MHz Varian INOVA spectrometer equipped with a magnetic field gradient probe. Signal postprocessing was performed with MestReC software.²³ The samples were prepared using $D_2\text{O}$ (99.9%), supplied by Aldrich, as solvent. The DOSY spectra were acquired with the standard stimulated echo pulse sequence using LED and bipolar gradient pulses. The gradient strengths (G) were changed from 2.1 to 64.3 G cm^{-1} in 20 steps, and the duration time of the gradient pulse (d) was kept constant at 2 ms. To obtain reliable results for the surfactant diffusion coefficient, the diffusion time (the time between leading edges of the field gradient pulses, Δ) was optimized for each sample to a value between 20 and 100 ms. The raw data were processed using the MestreC program (Mestrelab Research inc.). For molecules undergoing unhindered random motion and for a single species, the attenuation of the signal intensity is given by

$$I = I_0 \exp \left[-\gamma^2 G^2 \delta^2 \left(\Delta - \frac{\delta}{3} \right) D \right] \quad (2)$$

In eq 2, I denotes the observed intensity, I_0 is the intensity in the absence of gradient pulses, γ is the magnetogyric ratio, and the rest of the quantities are defined above. The experimental data were analyzed using a nonlinear least-squares fitting procedure (program Grafit 5.0, Erithacus Software Ltd.) to extract D from the observed monoexponential decay.

Phase scanning experiments were carried out using conventional slide-coverslip preparations and a BX51 polarized light microscope from Olympus, equipped with an Olympus DP71 digital video camera and software Cell-A for image acquisition.

Reaction kinetics was recorded by measuring the absorbance due to MBSC at 270 nm in a Cary 100 UV-vis spectrophotometer with a cell holder thermostated at $25.0 \pm 0.1^\circ\text{C}$. Stock solutions of MBSC were prepared in acetonitrile due to its low solubility in water. The final acetonitrile concentration in the reaction medium was 1% (v/v). The MBSC concentration was always approximately $1.2 \times 10^{-4} \text{ M}$. The absorbance-time data of all kinetic experiments were fitted by first-order integrated equations, and the values of the pseudo-first-order rate constants, k_{obs} , were reproducible to within 3%.

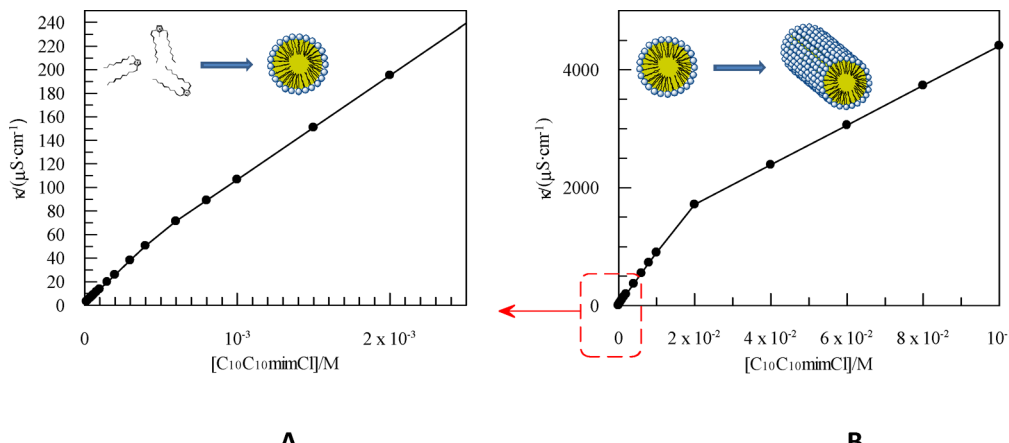


Figure 2. Specific conductivity (κ) of $[C_{10}C_{10}\text{mim}]Cl$ concentration in aqueous solution at 25 °C. (A) Range of $[C_{10}C_{10}\text{mim}]Cl$ concentrations between 1×10^{-5} and 2.5×10^{-3} M. (B) Range of $[C_{10}C_{10}\text{mim}]Cl$ concentrations between 1×10^{-5} and 0.1 M.

RESULTS AND DISCUSSION

1. UV-vis Spectroscopy. The physical properties of surfactant solutions show an abrupt change in the vicinity of a critical concentration due to the formation of molecular aggregates. A large number of experimental techniques can be applied to the determination of the critical micelle concentration (cmc).²⁴ One of them is UV-vis spectroscopy, which is based on the fact that the absorbance spectrum of many dyes added in very small amounts to a surfactant solution are different in the region below and above the cmc. The presence of aggregates leads to interactions with the dye that cause this change in the spectrum. The explanation is that the polarity in the interior of the micelle is very different from the polarity in bulk water, and hence, the dye, typically a hydrophobic molecule, tends to move to the aggregate core. The cmc value can be estimated from the plot of the wavelength of maximum absorbance (λ_{\max}) versus the surfactant concentration.

Reichardt developed an empirical polarity scale based on pyridinium N-phenolate betaine [$E_T(30)$].²⁵ In this study, we used a similar solvatochromic probe, $E_T(33)$, which was more suited to our system. Figure 1A shows the variation in E_T with $[C_{10}C_{10}\text{mim}]Cl$. The cmc can be detected from the slight decrease in E_T at 0.4 mM. Before the first micelles form, i.e., below the cmc, E_T remains constant. Increasing the concentration above the cmc, the E_T value decreases as a consequence of the incorporation of the probe molecule into the micellar pseudophase.

Comparing the E_T value of these IL micelles, $[C_{10}C_{10}\text{mim}]Cl \approx 0.1$ M, with the value in different solvents, one can see that the polarity is similar to that of the aliphatic alcohols methanol or 2-chloroethanol and higher than for ethanol.²⁵ With a comparative purpose, we carried out measurements of the influence of surfactant concentration on E_T for the common cationic surfactant tetradecyltrimethylammonium bromide (TTABr). In these cationic micelles, one observes an abrupt decrease in the E_T value above the cmc. For instance, Figure 1B shows this decrease in a small range of surfactant concentration, $(2.0-4.0) \times 10^{-3}$ M. The profile of the variation of E_T with surfactant concentration is very different in the case of the current IL and a wider range of concentrations (1.0×10^{-4} to 0.1 M) is required for a similar change in the polarity of micelle to take place. This behavior suggests a change in the structure of the IL aggregates, which as will be shown below is indeed detected by other techniques.

2. Conductimetry. Conductivity measurements of $[C_{10}C_{10}\text{mim}]Cl$ aqueous solutions are shown in Figure 2, where the specific conductivity (κ) is plotted as a function of $[C_{10}C_{10}\text{mim}]Cl$ concentration. As can be seen in Figure 2, there are three linear sections in the typical curves and the two slope changes are assigned to two different critical micelle concentrations.

In the literature, one can find several examples of two cmc values reported for surfactants.²⁶ Recently, the synthesis and self-aggregation in water of a hydroxyl-functionalized imidazolium-based IL surfactant, namely, 1-hydroxyethyl-3-dodecylimidazolium chloride ($[C_2\text{OHC}_{12}\text{im}]Cl$) has been studied.²⁷ Combined data from surface tension-concentration curves, fluorescence spectra, and electrical conductivity show that this IL has two cmc values. Surfactants tend to form small micelles in aqueous solutions at the cmc, but when the concentration is further increased, micellar growth can occur in some systems, and thus a shape transition from spheres to either rod-, thread-, worm-, or disk-like micelles. The first cmc value (cmc_1) corresponds to the formation of spherical micelles, and the second one (cmc_2) typically indicates the transition from spherical to rod-like micelles. We note here that thread- and worm-like micelles usually form at very high concentrations or in the presence of salt, organic counterion, or another cosolute, while disks are uncommon in single-surfactant systems.

In our system, the transition from IL unimers to spherical micelles corresponds to the first cmc (cmc_1) and can be obtained from the first change of the slope in the plots of κ vs IL concentration (Figure 2A). In a micelle, the mobility of the ions decreases and thus the electrical conductivity is lower than for free unimers. This cmc_1 value, at 25 °C (0.49 mM), is in agreement with the cmc value obtained from UV-vis measurements. Figure 2B shows the transition from small micelles to a solution containing elongated micelles, coexisting with the smaller ones, which defines the second cmc (cmc_2).²⁸ Rod-like micelles start to form at concentrations of IL above the cmc_2 (20 mM), and this change in the shape of the micelle leads to a change in the slope of the specific conductivity values of the system. In our system, the conductivimetric technique is more sensitive to the change of the shape of the micelles than the UV-vis that only allows us to determine cmc_1 .

The values of the fraction of surfactant counterions bound to the micelle (β_1 and β_2) can be obtained experimentally by determining the slope of the conductivity versus concentration

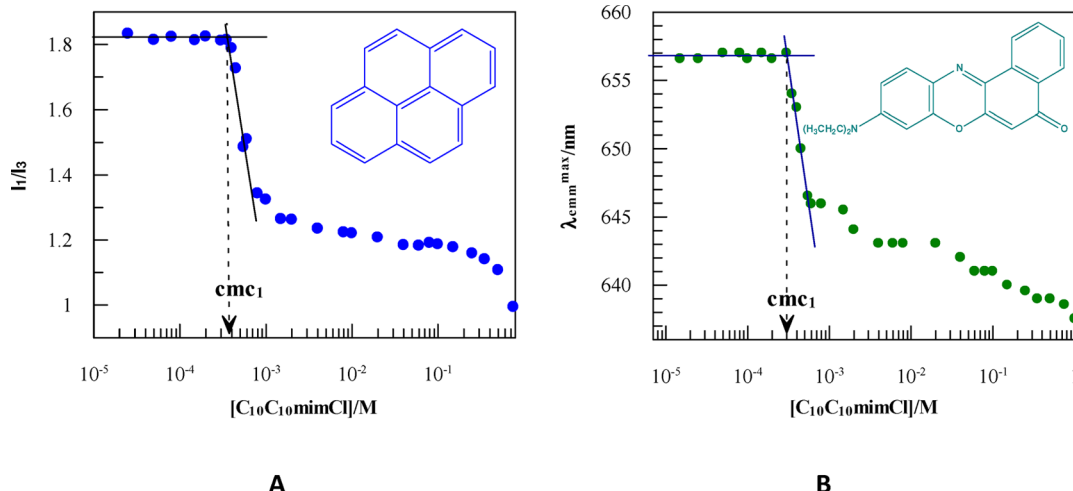


Figure 3. (A) Variation of the ratio I_1/I_3 of the emission spectrum of pyrene ($[\text{pyrene}] = 4 \times 10^{-7} \text{ M}$) with the concentration of $[C_{10}C_{10}\text{mim}]Cl$ in aqueous solution at 25°C . (B) Variation of the maximum wavelength of emission of Nile red ($[\text{Nile red}] = 1.6 \times 10^{-6} \text{ M}$) with the concentration of $[C_{10}C_{10}\text{mim}]Cl$ in aqueous solution at 25°C .

curves below and above cmc_1 and cmc_2 for spherical and rod-like micelles, respectively. According to traditional techniques used in the literature, the micelle ionization degree (α) can be obtained from the slopes of the conductivity vs surfactant concentration plots before and after the cmc. The degree of counterion binding can be determined from the micelle ionization degree through the relationship $\beta = 1 - \alpha$.¹⁶ The value of β is related to the charge density at the micelle surface.

Traditional ionic surfactants with long chains tend to aggregate in bulkier structures than shorter-chained surfactants and where the surface-to-volume ratio is smaller, and both the volume per surfactant ion and the number of ions per aggregate are larger. This means that the polar headgroups will be packed more closely and will be bound by a larger fraction of counterions. The result is a higher β value. However, if we have a double-chained surfactant, the values of β are lower with respect to single-chained surfactants of the same length. The presence of the second alkyl side chain leads to a decrease in the charge density at the surface of the micelle, and the headgroup penetrates a bit more into the core of the aggregate.²⁹ The β values for double-chained cationic surfactants with the formula $[C_nH_{2n+1}C_mH_{2m+1}N(CH_3)_2]Br$, referred to as C_nC_mDAB , have been previously calculated from microcalorimetric measurements or estimated from literature data.^{16,30} The β value decreases by increasing the length of the second chain, m , being, for example, 0.72, 0.56, 0.47, 0.38, and 0.26 for $C_{12}C_2DAB$, $C_{12}C_4DAB$, $C_{12}C_6DAB$, $C_{12}C_8DAB$, and $C_{12}C_{10}DAB$, respectively. The value of β_1 for $[C_{10}C_{10}\text{mim}]Cl$ is 0.28, being roughly in the same range as that of C_nC_mDAB surfactants. By increasing IL concentration, the packing of the polar headgroups becomes closer, leading to a change in the shape of the micelle. The value of β_2 is around 0.73, confirming that in rod-like micelles the polar headgroups are bound by a larger fraction of counterions than in spherical micelles.

3. Fluorescence Spectroscopy. Pyrene and Nile Red.

While cmc_1 can be obtained by many experimental methods, fewer ones have been employed to determine cmc_2 .³¹ In this instance, the steady-state spectrofluorimetric technique is a powerful tool to investigate both the first and second critical micelle concentrations of surfactants.³² In the present work, we used pyrene, Nile red, and rhodamine as fluorescent probes.

Pyrene is usually used as a fluorescent probe to investigate the polarity of the microenvironment of aggregates, on the basis of the fact that the molecule is very hydrophobic and hence it preferentially dissolves in the aggregate core. The emission spectrum of pyrene presents five vibration bands (see the Supporting Information). The intensity of the first band, I_1 , may be enhanced in a polar microenvironment, while the intensity of the third band, I_3 , is not sensitive to the surrounding environment. Consequently, the ratio of I_1/I_3 can be used both to estimate the polarity of the surfactant aggregates and to obtain the cmc of the surfactant in aqueous solution.³³ As shown in Figure 3A, the I_1/I_3 ratio remains constant on increasing IL concentration below cmc_1 (0.40 mM). When the first aggregates start to form, the I_1/I_3 ratio decreases with increasing surfactant concentration. The value of I_1/I_3 for spherical micelles (between cmc_1 and cmc_2) is around 1.20, similar to that of, for example, methanol or micelles of Brij35. At higher concentrations ($>10 \text{ mM}$), one observes a slight decrease in I_1/I_3 that indicates the presence of cmc_2 . This second transition is less clear than the first one, and cmc_2 cannot be estimated with precision.

Nile red exhibits a pronounced hydrophobic character, with low solubility and fluorescence emission in water. It is a good solvatochromic probe, and both steady-state and time-resolved emission properties are strongly medium-dependent.³⁴ For that reason, it has been extensively used to study micelles, microemulsions, or proteins.³⁵ Figure 3B shows how, at the lowest concentration of $[C_{10}C_{10}\text{mim}]Cl$ in water, there is no effect on maximum emission wavelength ($\lambda_{\text{em max}}$). Above cmc_1 ($\approx 0.30 \text{ mM}$), the maximum emission wavelength exhibits a blue shift, indicating that the micellar core provides a less polar environment than pure water. In addition, we do not obtain a constant value for the polarity of the micelle, which confirms that there is a change in the shape of the aggregates. A second slight decrease in $\lambda_{\text{em max}}$ can be detected at an IL concentration $>20 \text{ mM}$ and around this value starts the second transition from spherical micelles to rod-like ones. Anyway, cmc_2 is difficult to estimate with fluorescence probes.

Rhodamine B: Polarized Fluorescence Spectroscopy. The steady-state fluorescence anisotropy (r) is often used to predict the type of aggregates formed in aqueous solutions of various surfactants.³⁶ The probe molecule needs to be solubilized in the

hydrocarbon region of surfactant aggregates, and consequently, its rotational diffusion and hence fluorescence anisotropy are influenced by the fluidity of the microenvironment of the aggregates. The change in these properties can provide information on significant structural modifications in the system. The microviscosity of the interior of water-in-oil microemulsions has been examined by fluorescence depolarization experiments using sodium 3,4,9,10-perylenetetra-carboxylate,³⁷ rhodamine B,³⁸ or rhodamine 3B³⁹ as a fluorescent probe. Measurements of steady-state fluorescence anisotropy of rhodamine B can yield information on the microenvironmental properties of micelles.^{40,41} More recently, steady-state fluorescence depolarization experiments have been performed in different colloidal systems, for instance, to study the influence of α -cyclodextrin on the aggregation and interfacial properties of mixtures of nonionic and zwitterionic surfactants,⁴² to investigate the spontaneous formation of zwitterionic vesicles in zwitterionic/anionic surfactant mixtures⁴³ and to identify the micelle-to-gel transition of aqueous triblock copolymer solutions.⁴⁴

In this work, the fluorescence anisotropy value, r , was determined from the emission spectra of rhodamine B (eq 1). Figure 4 shows the variation of r with $[C_{10}C_{10}\text{mim}]Cl$ concentration.

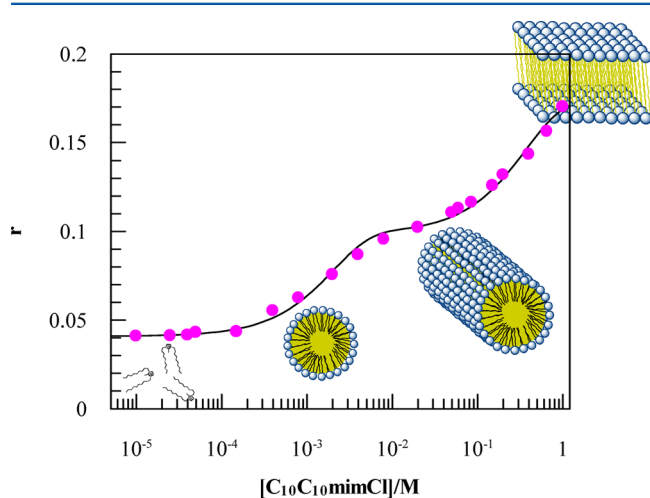


Figure 4. Variation in the fluorescence anisotropy (r) with $[C_{10}C_{10}\text{mim}]Cl$ concentration.

As can be seen, four different regions can be clearly identified in the plot. The first region ($[[C_{10}C_{10}\text{mim}]Cl] < 0.20 \text{ mM}$) corresponds to unimers of IL, the second one ($0.20 \text{ mM} < [[C_{10}C_{10}\text{mim}]Cl] < 40 \text{ mM}$) shows an r value in agreement with the presence of spherical micelles, and the third region ($[[C_{10}C_{10}\text{mim}]Cl] > 40 \text{ mM}$) is attributed to the change from spherical to cylindrical micelles. The r values >0.15 are tentatively assigned to bilayers appearing at the highest concentrations of IL. It has been reported that, for bilayer aggregates,⁴⁵ the fluorescence anisotropy of DPH is typically higher ($r > 0.14$) than that for spherical or rod-like micelles ($r < 0.14$).⁴³ This is because the hydrocarbon chains are more tightly packed in bilayer aggregates than in micelles and therefore the apolar microenvironment tends to be less fluid.

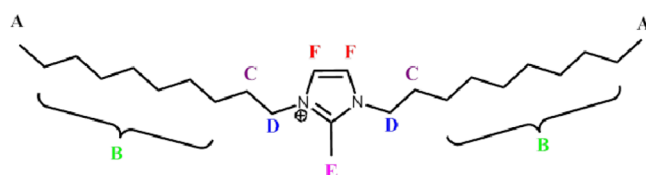
In summary, the fluorescence data from the probes pyrene, Nile red, and rhodamine B allow us to obtain values of cmc_1 (0.40, 0.30, and 0.20 mM) in agreement with the value obtained from conductivity (0.49 mM). The discrepancies arise

for the fact that in fluorescence spectroscopy we add probe molecules at the media and their different distribution in the aggregates can slightly modify the cmc_1 value. Moreover, fluorescence anisotropy measurements with rhodamine B are compatible with a cmc_2 value in the vicinity of 40 mM and introduce the possibility of a transition from micelles to bilayers for the highest concentrations of IL. In order to further confirm all of these results, NMR and light microscopy experiments were carried out and will be shown in the following sections.

4. NMR Spectroscopy: ¹H NMR and DOSY. ¹H NMR.

Since ¹H NMR chemical shift is sensitive to its local electronic environment, this technique allows us to obtain evidence for micelle formation.²⁶ The peak assignments of the ¹H NMR spectra of the IL (Scheme 2) in D₂O solution follow those well established in the literature and are shown in Figure 6.

Scheme 2



¹H NMR resonances for the hydrogen atoms of IL undergo reasonable chemical shifts as a function of the concentration. We can monitor the evolution of the chemical shifts in the ¹H NMR for the hydrogen atoms of surfactant headgroup as a function of the concentration by analyzing the difference between the chemical shifts for the unimer and the chemical shift at each concentration of IL. This can be conveniently defined here as $\Delta\delta = \delta_{\text{obs}} - \delta_{\text{unimer}}$, where δ_{unimer} is the value of δ when $[C_{10}C_{10}\text{mim}]Cl = 1.0 \times 10^{-4} \text{ M}$. The chemical shifts of the headgroup correspond to the signals of hydrogen atoms of the imidazolium ring (H_F) and those in the neighborhood of the ring (H_D and H_E).

The $\Delta\delta$ profiles for $[C_{10}C_{10}\text{mim}]Cl$ are shown in Figures 5 and S6 and S7 (Supporting Information), clearly suggesting the presence of a cmc_1 and cmc_2 . The cmc_1 value can be estimated as 0.4 mM and cmc_2 around 30–40 mM. The $\Delta\delta$ for these hydrogen atoms move to a lower field by increasing IL concentration. Shifting to a lower field for δ implies that the environment of the unimer molecules is changed, because of

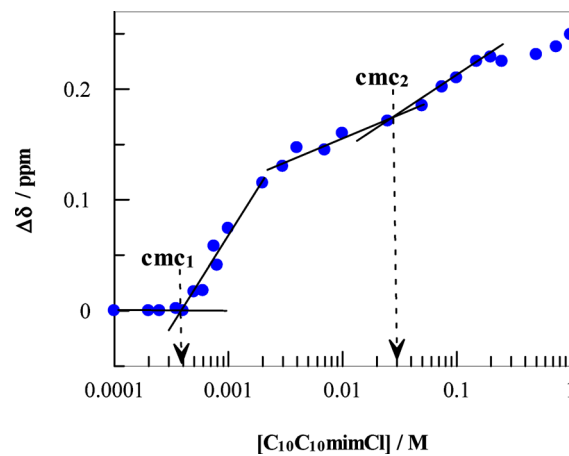


Figure 5. Variation of $\Delta\delta$ ($\Delta\delta = \delta_{\text{obs}} - \delta_{\text{monomer}}$) as a function of $[C_{10}C_{10}\text{mim}]Cl$ concentrations for H_D , $T = 25^\circ\text{C}$.

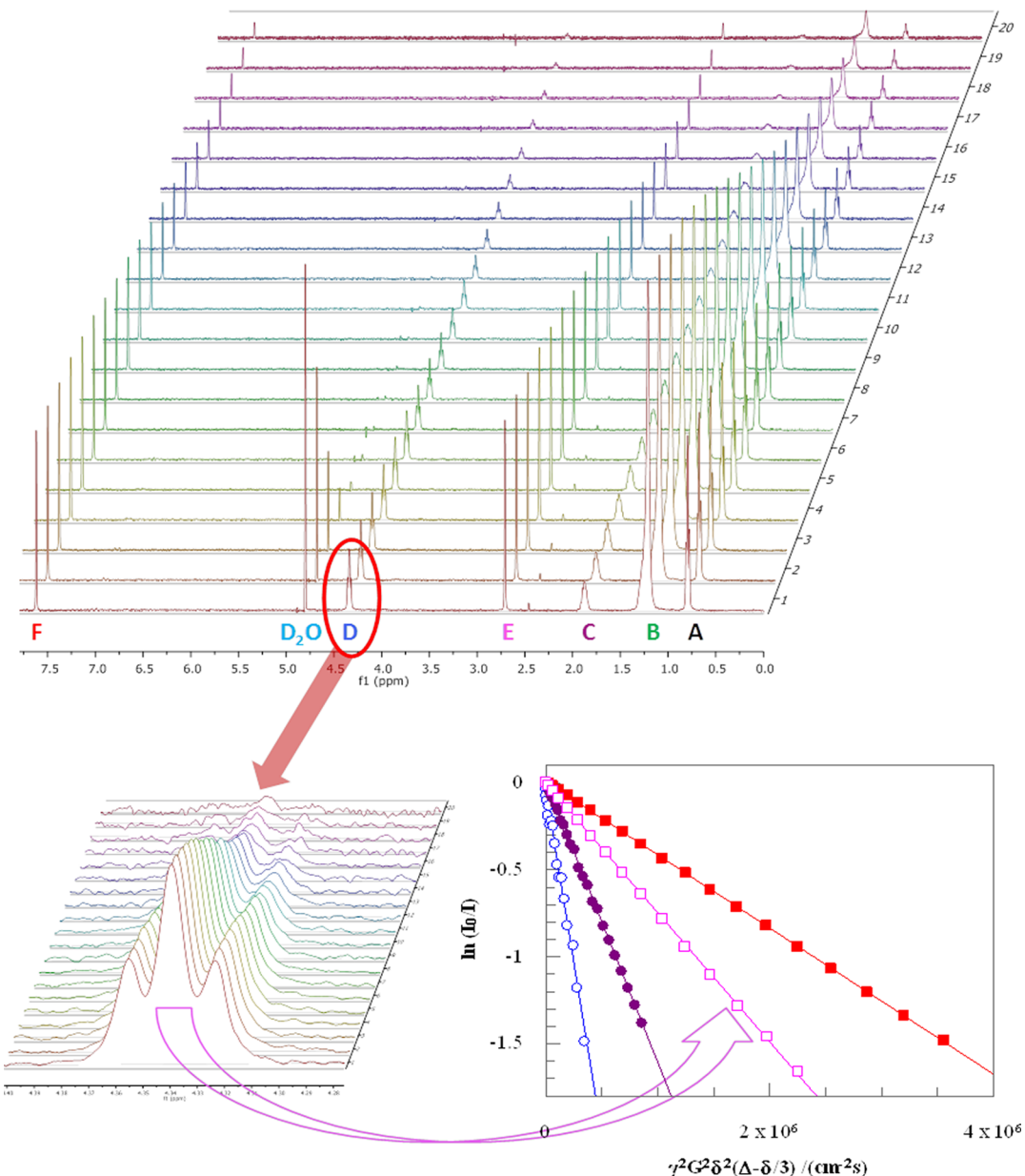


Figure 6. 500 MHz ^1H -DOSY display for a 50 mM solution of $[\text{C}_{10}\text{C}_{10}\text{mim}] \text{Cl}$ in D_2O at 25 °C. The left bottom figure shows a portion of the spectra that corresponds with the decay of the H_d hydrogen atoms of the IL. The right bottom graphic shows the linear signal attenuation of the H_d hydrogen atoms of $[\text{C}_{10}\text{C}_{10}\text{mim}] \text{Cl}$ against $(\gamma G\delta)^2(\Delta - \delta/3)$ using different diffusion times. The concentrations of IL in this graphic are 0.2 mM (○), 2 mM (●), 50 mM (□), and 100 mM (■). The lines show the fit of eq 2 to the experimental points.

the imidazolium current effect resulting from the association of unimers as the imidazolium rings come close together.⁴⁶

DOSY-NMR. The different diffusivity of unimers and aggregates can be used in order to obtain the cmc of the ionic liquid amphiphile. The self-diffusion coefficients allow us to estimate the critical micelle concentration, as well as the hydrodynamic radius of the aggregates distinguishing between spherical and cylindrical micelles.⁴⁷ The DOSY technique has also been used with IL surfactants to determine the cmc of pyridinium-based ILs¹² and oleate-based ILs²⁹ or to propose the existence of an ordered lamellar/micelle-based liquid crystal of ammonium-based Brønsted acid ILs.⁴⁸

Figure 6 shows an illustrative example of the ^1H NMR DOSY spectra of $[\text{C}_{10}\text{C}_{10}\text{mim}] \text{Cl}$. In this work, we used the H_d signals of the IL headgroup and D_2O hydrogen atoms for the

determination of the self-diffusion coefficients of IL and solvent, D_{obs} and $D_{\text{D}_2\text{O}}$, respectively. In all cases, clear monoexponential decays are obtained, suggesting that eq 2 (rearranged) can be applied. An example of a fit of eq 2 to the experimental data is shown in Figure 6. For further confirmation, the D_{obs} values were obtained using distinct diffusion times (Δ in eq 2), and the same value, within experimental error, was obtained.

As anticipated, the change in micellar size and shape can be inferred also from self-diffusion coefficient measurements. Figure 7 shows the variation in the self-diffusion coefficient of $[\text{C}_{10}\text{C}_{10}\text{mim}] \text{Cl}$ and D_2O (as reference) with amphiphile concentration. At lower IL concentrations, D_{obs} remains constant and corresponds to the diffusivity of free unimers. The formation of the first aggregates results in the apparent

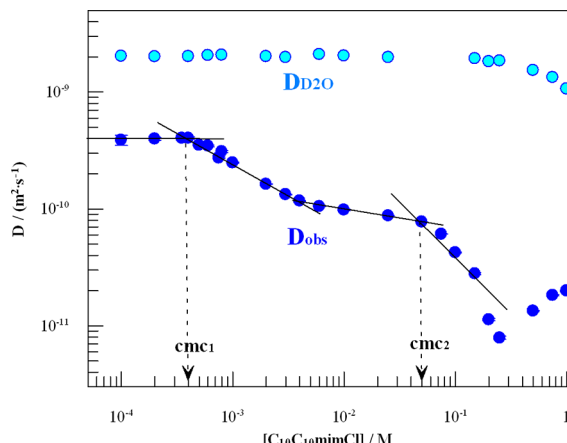


Figure 7. Variation of diffusion coefficient (D) as a function of $[C_{10}C_{10}\text{mim}]Cl$ concentrations for H_D proton, D_{obs} (royal blue circles), and $D_{D_2\text{O}}$ (turquoise circles), $T = 25^\circ\text{C}$.

self-diffusion coefficient decreasing slightly with the increase of concentration. The change in the slope can be assigned to cmc_1 (0.40 mM). Above cmc_1 , the D_{obs} is found to decrease, likely due to the growth of the spherical micelles to larger aggregates as the concentration increases. A second abrupt change of the slope is detected and can be assigned to cmc_2 (50 mM), corresponding to the transition from larger spherical micelles to cylindrical micelles. The slight discrepancy between the cmc values obtained from NMR (¹H NMR and DOSY) and those measured by different experimental techniques is attributed to a solvent effect, due to the known differences between $H_2\text{O}$ and $D_2\text{O}$.⁴⁹

Above cmc_1 , the surfactant molecules are in dynamic equilibrium between unimeric and micellar states. When the exchange kinetics is fast on the diffusion time scale, the observed diffusion coefficient for the IL (D_{obs}) is the molar fraction-weighted average of the diffusion coefficients of unimer (D_m) and micelle (D_M):

$$D_{\text{obs}} = x_m D_m + x_M D_M \quad (3)$$

where x_m and x_M are the molar fractions of $[C_{10}C_{10}\text{mim}]Cl$ in unimer state and in micelle state, respectively.

Using eq 3 along with the cmc_1 and D_m values (the average of D_{obs} obtained below cmc_1), it is possible to obtain the D_M value. In this work, we only calculated D_M for concentrations sufficiently above the cmc_1 to avoid any complications that could arise from the unimer–micelle exchange process. Once the D_M values are known, it is possible to calculate the effective hydrodynamic radius of the aggregates (r_h) using the Stokes–Einstein equation for spherical particles (discarding obstruction effects due to interparticle interactions):

$$D_M = \frac{k_b T}{6\pi\eta r_h} \quad (4)$$

where k_b is the Boltzmann constant, T the temperature, and η the viscosity of the solution.

Ionic micelle diffusivity depends on the surfactant and added electrolyte concentration. In a previous work, Galantini et al. using the DOSY technique studied the intermicellar interactions and micellar sizes in ionic micelle solutions.⁵⁰ In that work, the experimental data were analyzed by considering both the effect of micellar growth and interaction potential variation. They found that very slight micellar growth is induced by

increasing the added electrolyte and/or the surfactant concentration. The results were satisfactorily interpreted on the basis of the DLVO theory of colloid stability. At low ionic force, where the electrostatic repulsion dominates the interaction potential, the authors obtained similar results with a hard-core interaction model. In our system, the value of β_1 is 0.28 and this implies spherical micelles with a high charge resulting in relevant repulsive interactions among the micelles that affect their diffusion coefficient. In our data analysis, we do not take into account the previous considerations and the D_M value is slightly higher than the real self-diffusion coefficient of the micelle.

Between cmc_1 and cmc_2 , the calculated r_h values are typical of small micellar aggregates. We note that in view of the approximations made these calculated r_h values should be regarded as only qualitative, for example, for an IL concentration of 3 mM, a hydrodynamic radius of 2.2 nm. However, for concentrations of IL between 50 mM (cmc_2) and 250 mM, we observed an abrupt decrease in the D_M values, and as a result, the calculated equivalent r_h values increase from 2.7 to 27 nm. Simple calculations of the length of the unimeric unit of the $[C_{10}C_{10}\text{mim}]Cl$, using ChemOffice Chem3D, with the fully extended alkyl chain yield a value of 1.6 nm. Therefore, the calculated equivalent r_h values for the micellar aggregates are much higher than the surfactant length, suggesting that the micelles must have a nonspherical shape for this range of concentrations.

Finally, for the highest concentration of IL, one observes an increase in D_{obs} . This fact is surprising, if we take into account the combined effect of the viscosity of the media and interaggregate obstruction on the mobility of the aggregates. For IL concentrations below 0.2 M, the chemical shifts (Figure S.8, Supporting Information) and the diffusion coefficients of $D_2\text{O}$ (Figure 7) show no substantial variation with IL concentration, which proves that the contribution of the viscosity in the measured diffusion coefficients is small. For concentrations above 0.2 M, one observes a decrease in $D_{D_2\text{O}}$ as a consequence of the increased viscosity of the media. Thus, we can expect that this increase in viscosity can be reflected in a significant decrease in IL diffusion coefficient. However, we obtain an increase in the diffusion coefficient of the putative micelles (D_M). The reason for this behavior is that the surfactant diffusion measured at this concentration is influenced by the presence of bilayer aggregates, which arise in solution due to the existence of a lamellar liquid-crystalline phase at a much higher concentration of IL. Thus, the D_{obs} values are most likely influenced by the fast lateral diffusion of surfactant in the bilayers. We recall that these results are consistent with fluorescence anisotropy measurements, which already hinted at the presence of bilayers in the system. In order to obtain definitive evidence for this third structural evolution in the system (cylinders to bilayers), we carried out phase scanning experiments by polarized light microscopy.

5. Polarized Light Microscopy. The phase scanning experiment, in connection with polarized light microscopy, is a simple method that can provide invaluable qualitative information on the phase behavior of amphiphiles. The method is based on the formation of a surfactant concentration gradient upon controlled hydration of a powder sample.⁵¹ A drop of water is placed at one end of a coverslip and, by capillary action, seeps slowly into the solid film, showing the sequence of different phases. These are identified through characteristic

birefringent texture bands for anisotropic phases, or dark bands for isotropic phases, under plane-polarized light, allowing for a qualitative inspection of the phase diagram of the amphiphilic system.⁵²

With the aim of checking the phase behavior of $[C_{10}C_{10}\text{mim}]Cl$ beyond the micellar phase, a few different hydration essays were thus performed and the results are shown in Figure 8,

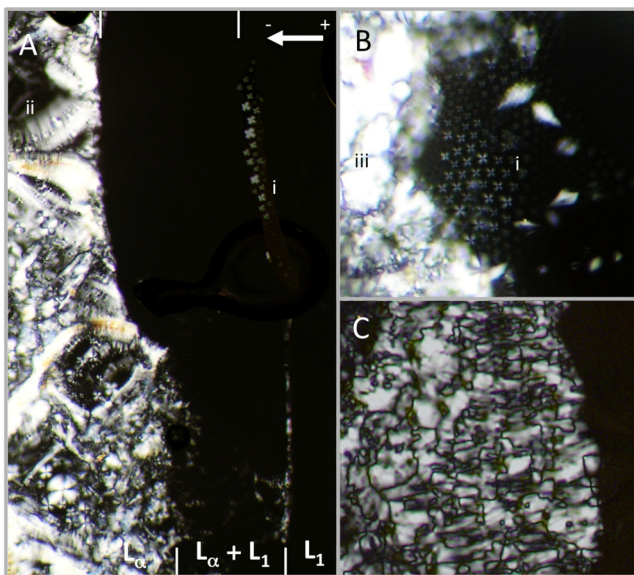


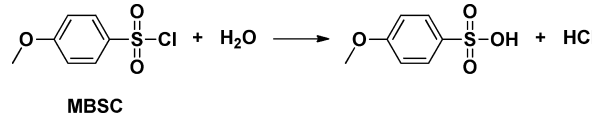
Figure 8. Polarized light micrographs of hydrated samples of $[C_{10}C_{10}\text{mim}]Cl$ in phase scanning experiments: (A) L_1 is the isotropic micellar phase (dark area) and L_ω lamellar liquid crystalline phase (texture), with oily streaks (i) and spherulitic focal conic domains or Maltese crosses (ii); (B) hydrated crystals to the left (iii) and Maltese crosses (i) forming close to the lamellar phase (appearing as a very narrow band here); (C) mosaic texture of the lamellar phase. The arrow in part A denotes the water gradient direction, which is the same in all images A–C.

where the water gradient goes right to left in all images. In Figure 8A, one can see as a first phase a wide isotropic liquid phase (dark area) corresponding to the micellar phase. On the left, a birefringent texture characteristic of a lamellar liquid crystalline phase (L_ω) is clearly formed. Several distinctive features for a L_ω phase are seen: focal conic domains (i) in Figure 8A and B, oily streaks (ii) in Figure 8A, and a mosaic-type texture (Figure 8C), all corresponding to different types of defects induced on the planar bilayer-structured phase that is confined between the slide and coverslip.⁵³ It is also possible to infer that this phase forms at very high amphiphile concentration, since it appears very close to the hydrated crystal region, which is seen in Figure 8B as an area of strong birefringence (iii). In Figure 8A, it is quite remarkable to see the large focal conic domains, also known as Maltese crosses, forming at what we interpret to be the boundary between the L_1 region and $L_1 + L_\omega$ two-phase region. In Figure 8B, they appear more randomly near the narrow lamellar texture and hydrated crystals. These crosses correspond to large spherical concentric bilayer domains ("onions") and are basically a spontaneously formed dispersion of L_ω domains in the liquid micellar phase. Hence, these are the bilayer structures captured previously by fluorescence anisotropy and self-diffusion NMR. They appear in the two-phase region $L_1 + L_\omega$ of the

$[C_{10}C_{10}\text{mim}]Cl$ -water system, where elongated micelles coexist with bilayer domains.

6. Chemical Reactivity: Solvolysis of MBSC. Chemical reactivity can be used in order to characterize a micellar system.⁵⁴ The kinetic studies in the presence of this type of aggregates are carried out for reactions where the reactants can be bonded to a micellar surface as a result of their hydrophobicity. To this end, we chose the hydrolysis reaction of 4-methoxybenzenesulfonyl chloride (MBSC, see Scheme 3).⁵⁵

Scheme 3



The absorbance-time data of all kinetic experiments were fitted by first-order integrated rate equations, and the values of the first order rate constants k_{obs} were reproducible to within 5%. The influence of the presence of the IL has been studied in a wide range of concentrations. For comparative purposes, Figure 9 shows the effect of surfactant concentration for the IL and octadecyltrimethylammonium chloride for the hydrolysis of MBSC. In the case of $[C_{10}C_{10}\text{mim}]Cl$, the k_{obs} value remains practically unchanged on increasing the IL concentration up until the cmc_1 . At surfactant concentrations higher than the cmc_1 , an abrupt decrease in k_{obs} can be observed due to the presence of micellar aggregates. From the change in the slopes, we can obtain a cmc_1 value (0.60 mM) slightly higher than the value obtained in the previous sections. The reason for this discrepancy is both the presence of acetonitrile in the reaction media, <1% (v/v), and the concentration of MBSC (1×10^{-4} M) in the same order of magnitude as cmc_1 .

If we analyze the influence of IL concentration on k_{obs} in the logarithmic scale, we can detect a second change in the slope that can be assigned to the cmc_2 value (30 mM).

The inhibition in the rate constant is a consequence of the MBSC incorporation into the micelles where the rate of the solvolytic reaction is smaller than that in bulk water. A deeper knowledge of the effect of this colloidal system on the solvolysis reaction can be reached by applying the formalism of the micellar pseudophase that allows us to obtain a quantitative interpretation of the experimental results.⁵⁶ In the pseudophase model, the rate effects are usually rationalized by considering that the aggregates and water are distinct reaction regions. The overall reaction rate is the sum of the rate in each pseudophase and depends on the rate constants and reactant concentrations in each pseudophase.

Initially, we can follow a traditional treatment for the kinetic experimental data through the pseudophase model assuming two pseudophases and discarding the change in the shape of the micelles that leads to the existence of cmc_2 . By considering that the solvolysis can take place simultaneously in water, k_w , and at the micellar pseudophase, k_m , it is possible to derive the following equation, which relates the observed rate constant with the surfactant concentration:

$$k_{\text{obs}} = \frac{k_w + k_m K_s [D_n]}{1 + K_s [D_n]} \quad (5)$$

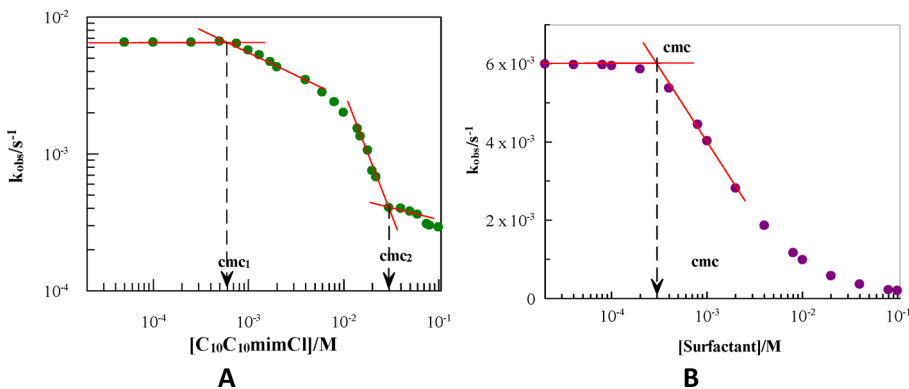


Figure 9. (A) Influence of $[C_{10}C_{10}\text{mimCl}]$ concentration on the pseudo-first-order rate constant (k_{obs}) for the hydrolysis of MBSC ($[\text{MBSC}] = 1 \times 10^{-4}$ M) at 25.0 °C. (B) Influence of octadecyltrimethylammonium chloride concentration on the pseudo-first-order rate constant (k_{obs}) for the hydrolysis of MBSC ($[\text{MBSC}] = 1 \times 10^{-4}$ M) at 25.0 °C.

where $[D_n]$ is the concentration of micellized surfactant, $[D_n] = [[C_{10}C_{10}\text{mimCl}]]_T - \text{cmc}_1$, and K_s is the distribution constant of MBSC between the water and the micellar pseudophases.

The values of cmc are required to fit eq 5 to the experimental results. The cmc_1 value can be obtained kinetically as the minimal surfactant concentration necessary to observe an appreciable change in k_{obs} (60 mM). The results obtained by fitting eq 5 to the experimental data are not satisfactory (see Figure 10) and lead us to consider the possibility of three pseudophases: water, cylindrical micelle, and spherical micelle (see Scheme 4).

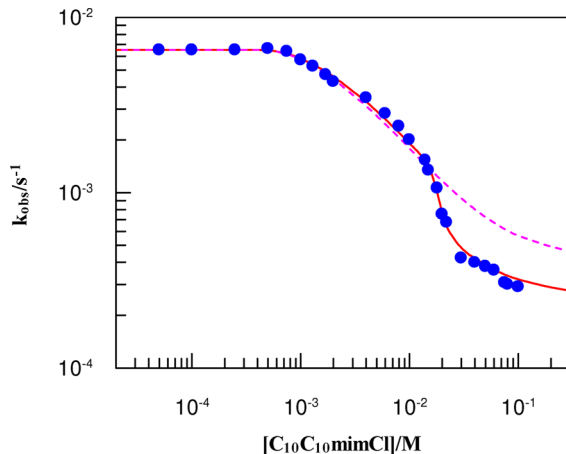


Figure 10. Influence of $[C_{10}C_{10}\text{mimCl}]$ concentration on the observed rate constant for the hydrolysis of MBSC ($[\text{MBSC}] = 1 \times 10^{-4}$ M) at 25.0 °C. The dotted fuchsia line represents the fit of the experimental data to eq 5. The solid red line represents the fit of the experimental data to eq 6.

A more detailed deduction of equations is shown in the Supporting Information, but on the basis of Scheme 3, we can obtain the following equation for k_{obs} :

$$k_{\text{obs}} = \frac{k_w + k_{m,1}K_{s,1}[D_{n,1}] + k_{m,2}K_{s,2}[D_{n,2}]}{1 + K_{s,1}[D_{n,1}] + K_{s,2}[D_{n,2}]} \quad (6)$$

where $k_{m,1}$ and $k_{m,2}$ are the rate constants in the spherical and cylindrical micelles, respectively, $K_{s,1}$ and $K_{s,2}$ are the distribution constants of MBSC between the three pseudophases, $D_{n,1}$ is the concentration of spherical micelles, and $D_{n,2}$ is the concentration of cylindrical micelles.

Scheme 4

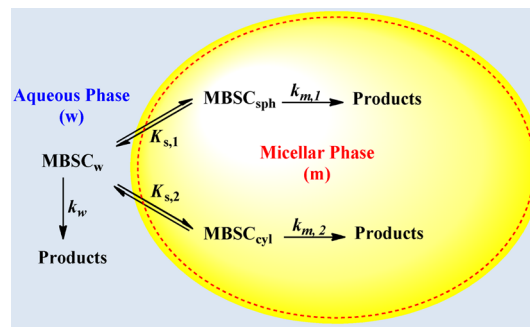


Figure 10 shows the excellent agreement between the experimental data and the calculated data from eq 6. From this fit, we obtained a value of $k_{m,1} = 4.0 \times 10^{-4}$ s^{-1} , $k_{m,2} = 2.5 \times 10^{-4}$ s^{-1} , $K_{s,1} = 320 \text{ M}^{-1}$, and $K_{s,2} = 900 \text{ M}^{-1}$. Our previous results obtained from fluorescence spectroscopy suggest that the change of shape of spherical to cylindrical micelles implies a decrease in the polarity of the micelle. The kinetic parameters obtained confirm this fact. The value of the association constant is larger for the cylindrical micelle than for the spherical one ($K_{s,2} > K_{s,1}$). This behavior is well documented in the literature as a consequence of the increase in the micelle hydrophobicity.⁵⁷ In the same way, for the solvolysis reaction, the rate constant decreases by decreasing the polarity of the media ($k_{m,2} < k_{m,1}$). Therefore, we can conclude that we have a new type of aggregates based on a double-chained IL that can be used as a novel reaction medium.

CONCLUSIONS

We have characterized the aggregation behavior of the ionic liquid 1,3-didecyl-2-methylimidazolium chloride in aqueous solution, finding a critical micelle concentration of about 0.4–0.5 mM (depending on the probing technique). This value is lower than the value for a surfactant with the same headgroup and a single chain or for a similar gemini surfactant. A second break point, at a concentration of 20–30 mM and designated as cmc_2 , is obtained as a consequence of a change in the shape and size of the micelles from spherical to cylindrical. Finally, at an even higher concentration of ionic liquid, a third structural evolution is detected, from cylindrical micelles to bilayer aggregates. These bilayer domains appear as a dispersion of a higher concentration lamellar phase in the micellar phase,

indicating a micelle–bilayer coexistence (two-phase region). The ability of this ionic liquid to form different types of micelle shapes was taken into account in the kinetic study of the solvolysis reaction of 4-methoxybenzenesulfonyl chloride.

■ ASSOCIATED CONTENT

Supporting Information

Examples of fluorescence and NMR experiments and a description of the pseudophase model for the kinetic study. This material is available free of charge via the Internet at <http://pubs.acs.org>.

■ AUTHOR INFORMATION

Corresponding Author

*E-mail: pedro.rodriguez@usc.es (P.R.-D.); luis.garcia@usc.es (L.G.-R.).

Notes

The authors declare no competing financial interest.

■ ACKNOWLEDGMENTS

This work was supported by the Ministerio de Ciencia y Tecnología (Project No. CTQ2011-22436) and Xunta de Galicia (PGIDIT10-PXIB209113PR and 2007/085). V.F. acknowledges FCT (Portugal) for Ph.D. grants SFRH/BD/43836/2008. E.F.M. is grateful to Centro de Investigação em Química da Universidade do Porto (CIQUP) for financial support through project Pest/C-QUI/UI0081/2011.

■ REFERENCES

- Rogers, R. D.; Voth, G. A. Ionic Liquids. *Acc. Chem. Res.* **2007**, *40*, 1077–1078.
- Kosmulski, M.; Gustafsson, J.; Rosenholm, J. B. Thermal Stability of Low Temperature Ionic Liquids Revisited. *Thermochim. Acta* **2004**, *412*, 47–53.
- Earle, M. J.; Esperança, J. M. S. S.; Gilea, M. A.; Canongia Lopes, J. N.; Rebelo, L. P. N.; Magee, J. W.; Seddon, K. R.; Widegren, J. A. The Distillation and Volatility of Ionic Liquids. *Nature* **2006**, *439*, 831–834.
- Fox, D. M.; Awad, W. H.; Gilman, J. W.; Maupin, P. H.; De Long, H. C.; Trulove, P. C. Flammability, Thermal Stability, and Phase Change Characteristics of Several Trialkylimidazolium Salts. *Green Chem.* **2003**, *5*, 724–727.
- Hallett, J. P.; Welton, T. Room-Temperature Ionic Liquids: Solvents for Synthesis and Catalysis. *2. Chem. Rev.* **2011**, *111*, 3508–3576.
- Van Rantwijk, F.; Sheldon, R. A. Biocatalysis in Ionic Liquids. *Chem. Rev.* **2007**, *107*, 2757–2785.
- MacFarlane, D. R.; Forsyth, M.; Howlett, P. C.; Pringle, J. M.; Sun, J.; Annat, G.; Neil, W.; Izgorodina, E. I. Ionic Liquids in Electrochemical Devices and Processes: Managing Interfacial Electrochemistry. *Acc. Chem. Res.* **2007**, *40*, 1165–1173.
- (a) Neuouze, M. A.; Le Bideau, J.; Gaveau, P.; Bellayer, S.; Vioux, A. Ionogels, New Materials Arising from the Confinement of Ionic Liquids within Silica-Derived Networks. *Chem. Mater.* **2006**, *18*, 3931–3936. (b) Balevicius, V.; Gdaniec, Z.; Aidas, K.; Tamuliene, J. NMR and Quantum Chemistry Study of Mesoscopic Effects in Ionic Liquids. *J. Phys. Chem. A* **2010**, *114*, 5365–5371. (c) Jones, Brad H.; Lodge, T. P. Hierarchically Porous Silica Prepared from Ionic Liquid and Polymeric Bicontinuous Microemulsion Templates. *Chem. Mater.* **2011**, *23*, 4824–4831.
- Zhao, H.; Jones, C. L.; Baker, G. A.; Xia, S.; Olubajo, O.; Person, V. N. Regenerating Cellulose from Ionic Liquids for an Accelerated Enzymatic Hydrolysis. *J. Biotechnol.* **2009**, *139*, 47–54.
- Blesic, M.; Marques, M. H.; Plechkova, N. V.; Seddon, K. R.; Rebelo, L. P. N.; Lopes, A. Self-Aggregation of Ionic Liquids: Micelle Formation in Aqueous Solution. *Green Chem.* **2007**, *9*, 481–490.
- Geng, F.; Liu, J.; Zheng, L.; Yu, L.; Li, Z.; Li, G.; Tung, C. Micelle Formation of Long-Chain Imidazolium Ionic Liquids in Aqueous Solution Measured by Isothermal Titration Microcalorimetry. *J. Chem. Eng. Data* **2010**, *55*, 147–151.
- Cornellas, A.; Perez, L.; Comelles, F.; Ribosa, I.; Manresa, A.; Garcia, M. T. Self-Aggregation and Antimicrobial Activity of Imidazolium and Pyridinium Based Ionic Liquids in Aqueous Solution. *J. Colloid Interface Sci.* **2011**, *355*, 164–171.
- Ding, Y.-S.; Zha, M.; Zhang, J.; Wang, S.-S. Synthesis, Characterization and Properties of Geminal Imidazolium Ionic Liquids. *Colloids Surf., A* **2007**, *298*, 201–205.
- Baltazar, Q. Q.; Chandawalla, J.; Sawyer, K.; Anderson, J. L. Interfacial and Micellar Properties of Imidazolium-Based Monocationic and Dicationic Ionic Liquids. *Colloids Surf., A* **2007**, *302*, 150–156.
- Pal, A.; Datta, S.; Aswal, V. K.; Bhattacharya, S. Small-Angle Neutron-Scattering Studies of Mixed Micellar Structures Made of Dimeric Surfactants Having Imidazolium and Ammonium Head-groups. *J. Phys. Chem. B* **2012**, *116*, 13239–13247.
- Zana, R. Ionization of Cationic Micelles: Effect of the Detergent Structure. *J. Colloid Interface Sci.* **1980**, *78*, 330–337.
- (a) Garcia Rio, L.; Cepeda, M.; Daviña, R.; Parajo, M.; Rodriguez-Dafonte, P.; Pessego, M. Competition Between Surfactant Micellization and Complexation by Cyclodextrin. *Org. Biomol. Chem.* **2013**, *11*, 1093–1102. (b) Jalali-Heravia, M.; Konouz, E. Multiple Linear Regression Modeling of the Critical Micelle Concentration of Alkyltrimethylammonium and Alkylpyridinium Salts. *J. Surfactants Deterg.* **2003**, *6*, 25–30.
- Roy, K.; Kabir, H. QSPR with Extended Topochemical Atom (ETA) Indices, 3: Modeling of Critical Micelle Concentration of Cationic Surfactants. *Chem. Eng. Sci.* **2012**, *81*, 169–178.
- Menger, F. M.; Keiper, J. S.; Azov, V. Gemini Surfactants with Acetylenic Spacers. *Langmuir* **2000**, *16*, 2062–2067.
- Lakowicz, J. *Principles of Fluorescence Spectroscopy*, 2nd ed.; Kluwer Academic/Plenum Publishers: New York, 1999.
- (a) Perrin, F. Polarization of Light of Fluorescence, Average Life of Molecules in the Excited State. *J. Phys. Radium* **1926**, *7*, 390–401. (b) Treloar, F. E. Fluorescence Depolarization Studies of the 1-Anilino-8-Naphthalene Sulfonate Anion in Glycerol-Water Mixtures. *Chem. Scr.* **1976**, *10*, 215–218.
- Carnero Ruiz, C. Fluorescence Anisotropy of Probes Solubilized in Micelles of Tetradecyltrimethylammonium Bromide: Effect of Ethylene Glycol Added. *J. Colloid Interface Sci.* **2000**, *221*, 262–267.
- Cobas, J. C.; Sardina, F. Nuclear Magnetic Resonance Data Processing. MestRe-C: A Software Package for Desktop Computers. *Concepts Magn. Reson., Part A* **2003**, *19A*, 80–96.
- Patist, A. *Handbook of Applied Surface and Colloidal Chemistry*; Holmberg, K., Ed.; Wiley-Blackwell: Chichester, U.K., 2001; Chapter 13, pp 239–249.
- Reichardt, C.; Welton, T. *Solvents and Solvent Effects in Organic Chemistry*, 4th, updated and enlarged ed.; Wiley-VCH Verlag & Co. KGaA: Weinheim, Germany, 2011.
- Qin, X.; Liu, M.; Zhang, X.; Yang, D. Proton NMR Based Investigation of the Effects of Temperature and NaCl on Micellar Properties of CHAPS. *J. Phys. Chem. B* **2011**, *115*, 1991–1998.
- Liu, X.-f.; Dong, L.-l.; Fang, Y. Synthesis and Self-Aggregation of a Hydroxyl-Functionalized Imidazolium-Based Ionic Liquid Surfactant in Aqueous Solution. *J. Surfactants Deterg.* **2011**, *14*, 203–210.
- Porte, G.; Poggi, Y.; Appel, J.; Maret, G. Large Micelles in Concentrated Solutions. The Second Critical Micellar Concentration. *J. Phys. Chem.* **1984**, *88*, 5713–5720.
- Tariq, M.; Podgorsek, A.; Ferguson, J. L.; Lopes, A.; Costa Gomes, M. F.; Pádua, A. A. H.; Rebelo, L. P. N.; Canongia Lopes, J. N. Characteristics of Aggregation in Aqueous Solutions of Dialkylpyrrolidinium Bromides. *J. Colloid Interface Sci.* **2011**, *360*, 606–616.
- Bai, G.; Wang, Y.; Yan, H.; Thomas, R. K. Enthalpies of Micellization of Double Chain and Gemini Cationic Surfactants. *J. Colloid Interface Sci.* **2001**, *240*, 375–377.

- (31) Zana, R. Critical Micellization Concentration of Surfactants in Aqueous Solution and Free Energy of Micellization. *Langmuir* **1996**, *12*, 1208–1211.
- (32) Romani, A. P.; Machado, A. E. H.; Hioka, N.; Severino, D.; Baptista, M. S.; Codognoto, L.; Rodrigues, M. R.; de Oliveira, H. P. M. Spectrofluorimetric Determination of Second Critical Micellar Concentration of SDS and SDS/Brij 30 Systems. *J. Fluoresc.* **2009**, *19*, 327–332.
- (33) Kalyansundaram, K.; Thomas, J. K. Environmental Effects on Vibronic Band Intensities in Pyrene Monomer Fluorescence and Their Application in Studies of Micellar Systems. *J. Am. Chem. Soc.* **1977**, *99*, 2039–2044.
- (34) (a) Deye, J. F.; Berger, T. A.; Anderson, A. G. Nile Red as a Solvatochromic Dye for Measuring Solvent Strength in Normal Liquids and Mixtures of Normal Liquids with Supercritical and Near Critical Fluids. *Anal. Chem.* **1990**, *62*, 615–622. (b) Dutt, G. B.; Doriswamy, S.; Periasamy, N. Molecular Reorientation Dynamics of Polar Dye Probes in Tertiary-Butyl Alcohol-Water Mixtures. *J. Chem. Phys.* **1991**, *94*, 5360–5368. (c) Dutt, G. B.; Doriswamy, S. Picosecond Reorientational Dynamics of Polar Dye Probes in Binary Aqueous Mixtures. *J. Chem. Phys.* **1992**, *96*, 2475–2491. (d) Cser, A.; Nagy, K.; Biczók, L. Fluorescence Lifetime of Nile Red as a Probe for the Hydrogen Bonding Strength with Its Microenvironment. *Chem. Phys. Lett.* **2002**, *360*, 473–478.
- (35) (a) Coutinho, P. J. G.; Castanheira, E. M. S.; Rei, M. C.; Real Oliveira, M. E. C. D. Nile Red and DCM Fluorescence Anisotropy Studies in C12E7/DPPC Mixed Systems. *J. Phys. Chem. B* **2002**, *106*, 12841–12846. (b) Maiti, N. C.; Krishna, M. M. G.; Britto, P. J.; Periasamy, N. Fluorescence Dynamics of Dye Probes in Micelles. *J. Phys. Chem. B* **1997**, *101*, 11051–11060. (c) Cicciarelli, B. A.; Hatton, T. A.; Smith, K. A. Dynamic Surface Tension Behavior in a Photoresponsive Surfactant System. *Langmuir* **2007**, *23*, 4753–4764. (d) Datta, A.; Mandal, D.; Pal, S. K.; Bhattacharyya, K. Intramolecular Charge Transfer Processes in Confined Systems. Nile Red in Reverse Micelles. *J. Phys. Chem. B* **1997**, *101*, 10221–10225. (e) Sackett, D. L.; Knutson, J. R.; Wol, J. *J. Biol. Chem.* **1990**, *265*, 14899–14906.
- (36) Nakashima, K.; Anzai, T.; Fujimoto, Y. Fluorescence Studies on the Properties of a Pluronic F68 Micelle. *Langmuir* **1994**, *10*, 658–661.
- (37) (a) Valeur, B.; Keh, E. Determination of the Hydrodynamic Volume of Inverted Micelles Containing Water by the Fluorescence Polarization Technique. *J. Phys. Chem.* **1979**, *83*, 3305–3307. (b) Keh, E.; Valeur, B. Investigation of Water-Containing Inverted Micelles by Fluorescence Polarization. Determination of Size and Internal Fluidity. *J. Colloid Interface Sci.* **1981**, *79*, 465–478.
- (38) (a) Wong, M.; Thomas, J. K.; Gratzel, M. Fluorescence Probing of Inverted Micelles. The State of Solubilized Water Clusters in Alkane/Diisooctyl Sulfosuccinate (Aerosol OT) Solution. *J. Am. Chem. Soc.* **1976**, *98*, 2391–2397. (b) Hasegawa, M.; Sugimura, T.; Suzuki, Y.; Shindo, Y.; Kitahara, A. Microviscosity in Water Pool of Aerosol-OT Reversed Micelle Determined with Viscosity-Sensitive Fluorescent Probe, Auramine O, and Fluorescence Depolarization of Xanthene Dyes. *J. Phys. Chem.* **1994**, *98*, 2120–2124.
- (39) Ferreira, J. A. B.; Costa, S. M. B. Electronic Excited-State Behavior of Rhodamine 3B in AOT Reverse Micelles Sensing Contact Ion Pair to Solvent Separated Ion Pair Interconversion. *J. Phys. Chem. B* **2010**, *114*, 10417–10426.
- (40) Carnero Ruiz, C.; Molina-Bolívar, J. A.; Aguiar, J.; MacIsaac, G.; Moroze, S.; Palepu, R. Thermodynamic and Structural Studies of Triton X-100 Micelles in Ethylene Glycol-Water Mixed Solvents. *Langmuir* **2001**, *17*, 6831–6840.
- (41) Hierrezuelo, J. M.; Aguiar, J.; Carnero Ruiz, C. Stability, Interaction, Size, and Microenvironmental Properties of Mixed Micelles of Decanoyl-N-methylglucamide and Sodium Dodecyl Sulfate. *Langmuir* **2004**, *20*, 10419–10426.
- (42) Sehgal, P.; Mizuki, T.; Doe, H.; Wimmer, R.; Larsen, K. L.; Otzen, D. E. Interactions and Influence of α -Cyclodextrin on the Aggregation and Interfacial Properties of Mixtures of Nonionic and Zwitterionic Surfactants. *Colloid Polym. Sci.* **2009**, *287*, 1243–1252.
- (43) Ghosh, S.; Khatua, D.; Dey, J. Interaction Between Zwitterionic and Anionic Surfactants: Spontaneous Formation of Zwitterionic Vesicles. *Langmuir* **2011**, *27*, 5184–5192.
- (44) George, S.; Kumbhakar, M.; Singh, P. Kr.; Ganguly, R.; Nath, S.; Pal, H. Fluorescence Spectroscopic Investigation To Identify the Micelle to Gel Transition of Aqueous Triblock Copolymer Solutions. *J. Phys. Chem. B* **2009**, *113*, 5117–5127.
- (45) Roy, S.; Mohanty, A.; Dey, J. Microviscosity of Bilayer Membranes of Some N-Acylamino Acid Surfactants Determined by Fluorescence Probe Method. *Chem. Phys. Lett.* **2005**, *414*, 23–27.
- (46) Cui, X.; Mao, S.; Liu, M.; Yuan, H.; Du, Y. Mechanism of Surfactant Micelle Formation. *Langmuir* **2008**, *24*, 10771–10775.
- (47) Angelico, R.; Ceglie, A.; Colafemmina, G.; Lopez, F.; Olsson, U.; Palazzo, G. Biocompatible Lecithin Organogels: Structure and Phase Equilibria. *Langmuir* **2005**, *21*, 140–148.
- (48) (a) Alvarez, V. H.; Dosil, N.; Gonzalez-Cabaleiro, R.; Mattedi, S.; Martin-Pastor, M.; Iglesias, M.; Navaza, J. M. Brønsted Ionic Liquids for Sustainable Processes: Synthesis and Physical Properties. *J. Chem. Eng. Data* **2010**, *55*, 625–632. (b) Alvarez, V. H.; Mattedi, S.; Martin-Pastor, M.; Aznar, M.; Iglesias, M. Synthesis and Thermo-physical Properties of Two New Protic Long-Chain Ionic Liquids with the Oleate Anion. *Fluid Phase Equilib.* **2010**, *299*, 42–50.
- (49) Basilio, N.; García-Río, L.; Martín-Pastor, M. NMR Evidence of Slow Monomer-Micelle Exchange in a Calixarene-Based Surfactant. *J. Phys. Chem. B* **2010**, *114*, 4816–4820.
- (50) Galantini, L.; Giampaolo, S. M.; Mannina, L.; Pavel, N. V.; Viel, S. Study of Intermicellar Interactions and Micellar Sizes in Ionic Micelle Solutions by Comparing Collective Diffusion and Self-Diffusion Coefficients. *J. Phys. Chem. B* **2004**, *108*, 4799–4805.
- (51) (a) Lawrence, A. S. C. Lyotropic Mesomorphism in Lipid-Water System. *Mol. Cryst. Liq. Cryst.* **1969**, *7*, 1–57. (b) Laughlin, R. G. *The Aqueous Phase Behavior of Surfactants*; Academic Press Limited: London, 1994.
- (52) Oliveira, I. M. S. C.; Silva, J. P. N.; Feitosa, E.; Marques, E. F.; Castanheira, E. M. S.; Real Oliveira, M. E. C. D. Aggregation Behavior of Aqueous Dioctadecyltrimethylammonium Bromide/Monoolein Mixtures: A Multitechnique Investigation on the Influence of Composition and Temperature. *J. Colloid Interface Sci.* **2012**, *374*, 206–217.
- (53) Rades, T.; Müller-Goyman, C. C. Electron and Light Microscopical Investigation of Defect Structures in Mesophases of Pharmaceutical Substances. *Colloid Polym. Sci.* **1997**, *275*, 1169–1178.
- (54) (a) Marte, L.; Beber, R. C.; Farrukh, M. A.; Micke, G. A.; Costa, A. C. O.; Gillitt, N. D.; Bunton, C. A.; Di Profio, P.; Savelli, G.; Nome, F. Specific Anion Binding to Sulfobetaine Micelles and Kinetics of Nucleophilic Reactions. *J. Phys. Chem. B* **2007**, *111*, 9762–9769. (b) Priebe, J. P.; Souza, B. S.; Micke, G. A.; Costa, A. C. O.; Fiedler, H. D.; Bunton, C. A.; Nome, F. Anion-Specific Binding to n-Hexadecyl Phosphorylcholine Micelles. *Langmuir* **2010**, *26*, 1008–1012.
- (55) (a) García-Río, L.; Méndez, M.; Paleo, M. R.; Sardina, F. J. New Insights in Cyclodextrin: Surfactant Mixed Systems from the Use of Neutral and Anionic Cyclodextrin Derivatives. *J. Phys. Chem. B* **2007**, *111*, 12756–12764. (b) Cepeda, M.; Davina, R.; Garcia-Río, L.; Parajo, M. Cyclodextrin-Surfactant Binding Constant as Driven Force for Uncomplexed Cyclodextrin in Equilibrium with Micellar Systems. *Chem. Phys. Lett.* **2010**, *499*, 70–74.
- (56) García-Río, L.; Hervés, P.; Mejuto, J. C.; Pérez-Juste, J.; Rodríguez-Dafonte, P. Comparative Study of Nitroso Group Transfer in Colloidal Aggregates: Micelles, Vesicles and Microemulsions. *New J. Chem.* **2003**, *27*, 372–380.
- (57) Bunton, C. A. Micellar Charge Effects as Mechanistic Criteria in Spontaneous Hydrolyses of Acid Chlorides. *J. Phys. Org. Chem.* **2005**, *18*, 115–120.